Received: 13 June 2020 | Revised: 7 August 2020 | Accepted: 11 September 2020

DOI: 10.1002/ardp.202000199

FULL PAPER

DPhG ARCH PHARM Archiv der Pharmazie

Synthesis, in vitro antibacterial activity against *Mycobacterium tuberculosis*, and reverse docking-based target fishing of 1,4-benzoxazin-2-one derivatives

Ekaterina E. Stepanova | Svetlana Yu. Balandina | Vera A. Drobkova | Maksim V. Dmitriev | Irina V. Mashevskaya | Andrey N. Maslivets

Department of Chemistry, Perm State University, Perm, Russia

Correspondence
Ekaterina E. Stepanova and Andrey N. Maslivets, Department of Chemistry, Perm State University, ul. Bukireva 15, Perm, Russian Federation, 614990.
Email: caterina.stepanova@psu.ru (E. E. S.) and koh2@psu.ru (A. N. M.)

Funding information
Government of Perm Krai; Ministry of Science and Higher Education of the Russian Federation, Grant/Award Number: FSNF-2020-0008

Abstract

Seventeen 1,4-benzoxazin-2-ones bearing the enaminone moiety and three of their analogs were tested for the antibacterial activity against *Mycobacterium tuberculosis* (H37Rv). Minimal bactericidal concentrations (MBCs) were determined after 41 days of incubation by BACTEC. 1,4-Benzoxazin-2-ones bearing the unsubstituted benzo moiety showed the most promising activities (MBC = 5.00 μg/ml). For most active compounds, antibacterial activities were determined daily during the 41 days. The most promising compound showed a bacteriostatic effect at a concentration of 0.31 μg/ml on Day 4 of incubation, 0.62 μg/ml on Day 6, 2.50 μg/ml on Day 9, and 5.00 μg/ml on Day 41. All studied compounds, along with some of their reported analogs, were docked to 35 proteins of *M. tuberculosis* to find their potent targets in these organisms. As a result of reverse docking, aspartate 1-decarboxylase, *panD*, was selected as the most appropriate target. Docking of the most active compounds to mutant *panD* from pyrazinamide-resistant strains of *M. tuberculosis* implies that they would not be active against these strains. Considering that most of pyrazinamide clinical resistance cases are due to loss-of-function mutations in pyrazinamidase, *pncA*, compounds from this study could be useful drugs for the treatment of some cases of pyrazinamide-resistant tuberculosis.

KEYWORDS

1,4-benzoxazin-2-one, antibacterial activity, molecular docking, *Mycobacterium tuberculosis*, *panD*

1 | INTRODUCTION

Tuberculosis (TB) is a communicable disease that is one of the top 10 causes of death worldwide and the leading cause of death from a single infectious agent. Overcoming the global public health crisis of multidrug-resistant TB requires incessant search for new anti-TB agents.

Anti-TB drug development is complicated by the nature of the TB pathogen, *Mycobacterium tuberculosis* (*Mtb*), which is characterized by slow growth and high pathogenicity.[1] In addition, it is important to consider economic factors, as TB treatment duration is about 6 months, which imposes a serious economic burden both for the patient and the state.

1,4-Benzoxazin-2-ones bearing the enaminone moiety (BOs; Figure 1) have been thoroughly investigated for various biological activities (antioxidant,[2] antimicrobial,[3,4] antimycotic,[3,5] anti-Alzheimer's disease,[6] platelet aggregation inhibitory,[7] and antimycobacterial[8,9]), as they are attractive platforms for the development of inexpensive drugs due to the simplicity of their synthesis and purification, the availability of starting materials, and the possibility of their synthesis under mild green conditions in gram-scale quantities.[2,10–12]

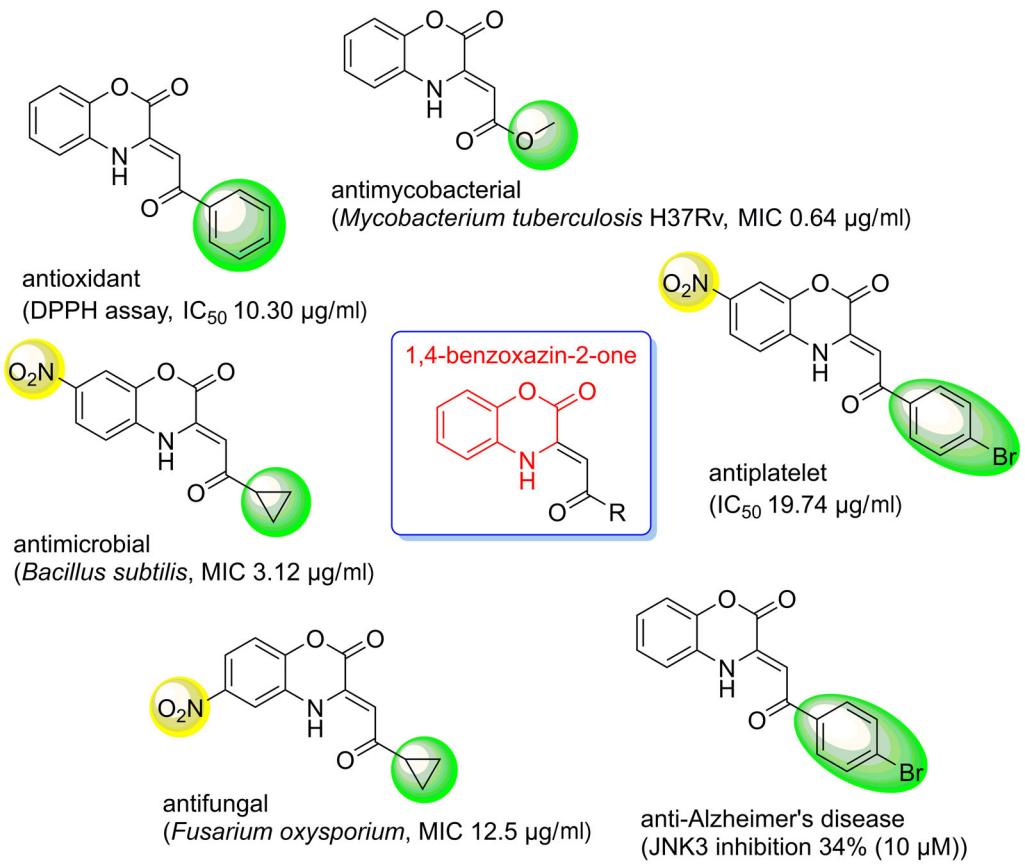

FIGURE 1 1,4-Benzoxazin-2-ones bearing the enaminone moiety

Recently, BOs were found to exhibit significant antibacterial activity against *Mtb*.[8,9] Detailed studies of structure–activity relationships (SAR) of these compounds and their analogs (isosteres and open-ring analogs) were performed.[8,9]

BOs examined for anti-TB activity[8,9] belong to two chemically different groups of enaminones, aroyl (R = Ar, Figure 1) and alkoxycarbonyl-bearing ones (R = OAlk, Figure 1). One more group of BOs, alkyloyl-bearing ones (R = Alk, Figure 1), was not investigated in whole-cell assays for the antibacterial activity against *Mtb*, despite the fact that it was the first to be identified in high-throughput screen as *MenB*, 1,4-dihydroxy-2-naphthoyl-CoA synthase, inhibitors for the development of new anti-TB agents.[8]

Herein, we report a study on the anti-TB activity of undervalued BOs bearing the alkyloyl (R = *tert*-Bu, *iso*-Bu, Figure 1) substituents and reverse docking evaluation of their potent targets in cells of *Mtb*.

2 | RESULTS AND DISCUSSION

2.1 | Chemistry

Methoxycarbonyl-bearing BO **1a**, which was reported as an anti-TB hit compound by Li et al.,[8] was synthesized by the reaction of dimethyl acetylenedicarboxylate (DMAD) with *o*-aminophenol **2a** (Scheme 1). BO **1a** was necessary as a starting point and a reference compound for our study of evaluation of anti-TB properties of novel BOs and their analogs.

Ethoxycarbonyl-bearing BOs **1b,c** were synthesized by the condensation of diethyl oxaloacetate **3a** with *o*-aminophenols **2a,b** (Scheme 2).

Alkyloyl-bearing BOs **1c–p** were synthesized by the condensation of methyl acylpyruvates **3b,c** with *o*-aminophenols **2a–h** (Scheme 3). According to a similar procedure (Scheme 3), their 4-fluorophenyl analog, BO **1q**, was synthesized, starting from methyl 4-fluorobenzoylpyruvate **3d**.

In addition, to expand the chemical space around target BO **3**, we designed its novel open-ring analog, enamine **4**; it was synthesized by

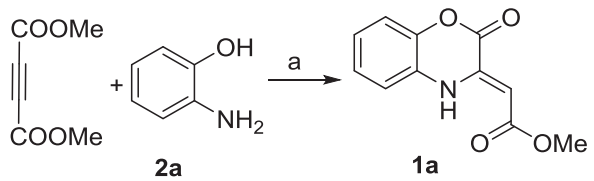

SCHEME 1 The synthesis of methoxycarbonyl-bearing BO **1a**. Reagents and conditions: (a) MeOH, rt, 24 hr

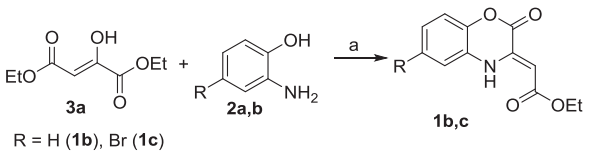

SCHEME 2 The synthesis of ethoxycarbonyl-bearing BOs **1b,c**. Reagents and conditions: (a) EtOH, reflux, 5 min

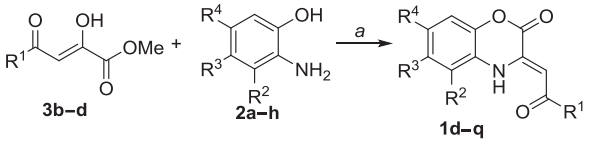

SCHEME 3 The synthesis of BOs **1d–q**. Reaction and reagents: (a) EtOH, reflux, 5 min

condensation of diethyl oxaloacetate **3a** with *N*-(2-aminophenyl) acetamide (Scheme 4).

Finally, we planned to study the anti-TB activity of annelated analogs of BO **1**, pyrrolobenzoxazines **5a,b**. They were prepared by acylation of BOs **1b,q** with oxalyl chloride (Scheme 5).[13,14] It should be considered that pyrrolobenzoxazines **5a,b** readily undergo hydrolysis (Scheme 5),[15] which is easy to notice by the color change (dark violet to yellow) when dissolved in media containing water. In fact, the anti-TB activity of pyrrolobenzoxazines **5a,b** is not investigated; however, the anti-TB activity of their hydrolysis products, **6a,b**, is investigated.

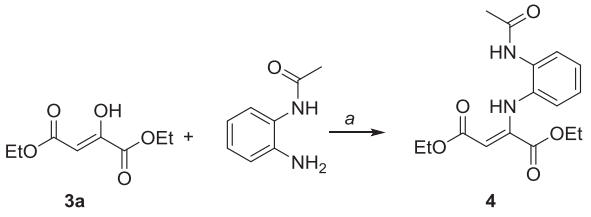

SCHEME 4 The synthesis of the open-ring analog of BO **1**, enamine **4**. Reaction and reagents: (a) EtOH, reflux, 5 min

2.2 | Pharmacology/Biology

A series of 20 synthesized compounds was tested for activity against pathogenic *Mtb* (H37Rv) using the standard BACTEC radiometric growth assay. The effect of test compounds on the growth of *Mtb* was monitored on Day 41. The lowest dilutions of the examined compounds, in which no growth of *Mtb* was detected by BACTEC on Day 41 of the assay, were considered as minimal bactericidal concentrations (MBCs; Table 1).

On Day 41, 8 of 20 examined compounds were found to exhibit a significant bactericidal activity against *Mtb*. Control tubes, containing growth media, *Mtb*, and no test compounds, showed abundant growth of mycobacteria.

The highest mycobactericidal activity was shown by compounds having no substituents in 1,4-benzoxazine moiety, BOs **1b,d,l,q**, at a concentration of 5.0 μg/ml, which is in agreement with previous SAR studies of BOs.[8,9] Unexpectedly, BO **1a**, reported earlier as an anti-TB hit compound,[8] did not fall into the group of the most active compounds and showed a bactericidal effect at a concentration of 10 μg/ml. In our assay, replacement of methyl in compound **1a** for ethyl (compound **1b**) resulted in an increase of bactericidal activity, that is, MBC of methyl-bearing compound **1a** was 10 μg/ml and MBC of ethyl-bearing compound **1b** was 5 μg/ml.

Compound **1k**, bearing 6-Cl substituent in 1,4-benzoxazine moiety, showed a bactericidal effect at a concentration of 10 μg/ml. Compounds **1m,p**, bearing 6-halogen (Br and Cl) substituents in 1,4-benzoxazine moiety, showed a mycobactericidal activity at a concentration of 20 μg/ml, and compound **1c**, a 6-Br analog of BO **1b**, did not show a bactericidal effect. The introduction of methyl- and nitro-substituents in 1,4-benzoxazine moiety deteriorated the antibacterial activity of BOs **1f,g,i,j,n,o**. The same effect had a benzo-substituent in 1,4-benzoxazine moiety of BO **1e**. This confirms that unsubstituted 1,4-benzoxazine moiety is crucial for anti-TB activity.

Annelated analogs of BOs, compounds **5a,b**, and the open-ring analog of BOs, enamine **4**, did not show bactericidal activity.

Incorporation of an alkyloyl substituent in BO **1** did not result in the degradation of anti-TB activity. A similar effect of incorporation of 4-fluorobenzoyl substituent was observed.

The examined *tert*-Bu and *iso*-Bu substituents in BO **1** showed a similar effect on the anti-TB activity. But simultaneous changes both in alkyloyl substituents and 6-halogen ones resulted in different effects. So, for 6-Cl-substituted BOs, *tert*-Bu-bearing BO **1k** showed a bactericidal effect at a concentration of 10 μg/ml, and its *iso*-Bu analog, BO **1m**, showed a bactericidal effect at a concentration of 20 μg/ml.

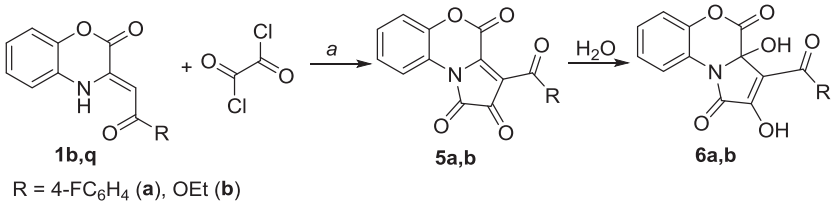

SCHEME 5 Synthesis and hydrolysis of annelated analogs of BO **1**, pyrrolobenzoxazinones **5a,b**. Reaction and reagents: (a) Benzene, reflux, 90 min

TABLE 1 Results of the anti-TB assay by BACTEC

Entry	Compound	Structure	MBC (μg/ml)[a]
1	**1a**	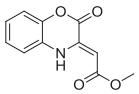	10
2	**1b**	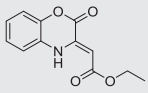	5
3	**1c**	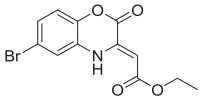	>20
4	**1d** (CCDC 2005170)	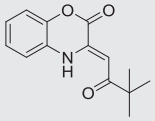	5
5	**1e**	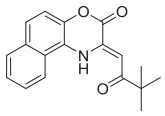	>20
6	**1f**	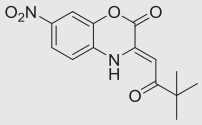	>20
7	**1g**	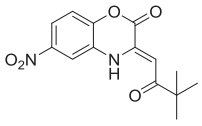	>20
8	**1h**	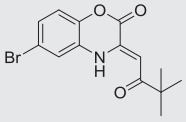	>20
9	**1i**	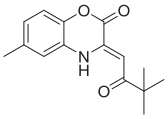	>20
10	**1j**	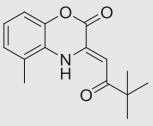	>20
11	**1k**	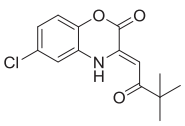	10
12	**1l**	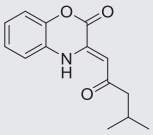	5
13	**1m**	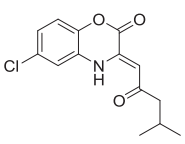	20

TABLE 1 (Continued)

Entry	Compound	Structure	MBC (μg/ml)[a]
14	**1n**	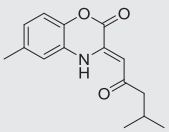	>20
15	**1o**	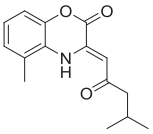	>20
16	**1p**	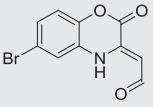	20
17	**1q**	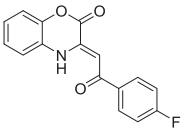	5
18	**4**	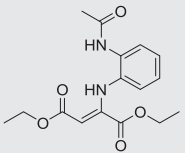	>20
19	**5a**	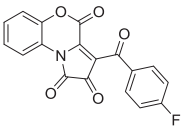	>20
20	**5b**	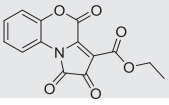	>20
21	Isoniazid	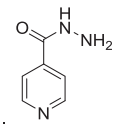	1.25

Abbreviations: MBC, minimal bactericidal concentration; TB, tuberculosis.

[a]The lowest dilution of the examined compound in which no bacterial growth was detected on Day 41 of the assay.

Compounds with the highest anti-TB activity were additionally tested by BACTEC, which detected the presence or absence of growth of mycobacteria daily for 41 days (Figure 2). During the assay, the growth rate of *Mtb* was compared in the control tube and in tubes with a certain concentration of test substances.

According to Figure 2, the studied compounds **1b,d,l,q** had a pronounced bactericidal effect against mycobacteria at a quite low concentration of 5 μg/ml. At this concentration, the compounds completely inhibited the growth of the TB pathogens, and the culture growth was not observed throughout the incubation time. In control tubes (medium containing *Mtb*), abundant growth of mycobacteria was observed on the fourth day of the assay.

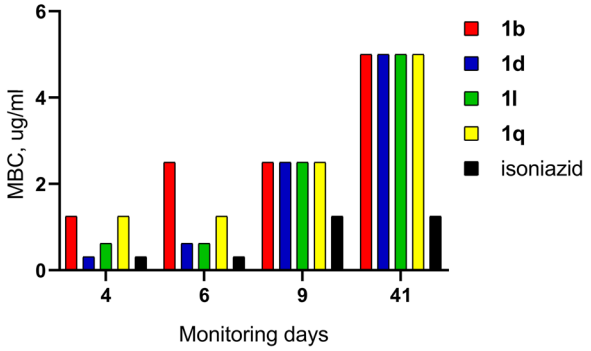

FIGURE 2 Results of the antituberculosis assay by BACTEC (the lowest dilution of the examined compound in which no bacterial growth was detected on the monitoring day; the growth was detected on Day 4 in control tubes without test compounds). MBC, minimal bactericidal concentration

Alkyloyl-bearing compounds **1d,l** exhibited a bacteriostatic effect at the lowest concentration of 0.62 μg/ml on the *Mtb* during the first 6 days of the assay. Considering the slightly better effect of compound **1d** on the fourth day, it can be concluded that BO **1d** is a better candidate for drug development.

Selected BOs **1d,k,q** were tested by resazurin microtiter assay (REMA)[16,17] for anti-TB activity (Table 2). The results were monitored on Day 10, which were generally in agreement with the results of BACTEC assay; the same SARs were observed. BOs **1d,q**, bearing no substituents in 1,4-benzoxazine moiety, showed the lowest minimum inhibition concentrations (MICs) of 0.97 μg/ml. Compound **1k**, bearing 6-Cl substituent in 1,4-benzoxazine moiety, showed MIC at a higher concentration of 7.8 μg/ml.

2.3 | Molecular docking

Identification of a target from a variety of candidate macromolecules is a challenging task. Out of 890 known metabolic genes of *Mtb*, structural data for only 140 of them are deposited in the structural database PDB.[18]

To conjecture a potent target for BO **1**, we used a reverse docking strategy. For this purpose, we prepared a library of targets of *Mtb* (H37Rv), based on a review by H. Tomioka et al.,[] summarizing promising targets for anti-TB drug discovery (Table 3).

TABLE 2 Results of the anti-TB assay by REMA

Entry	Compound	MIC (μg/ml)
1	**1d**	0.97
2	**1k**	7.8
3	**1q**	0.97
4	Isoniazid	0.032

Abbreviations: MIC, minimum inhibition concentration; REMA, resazurin microtiter assay; TB, tuberculosis.

Performing the reverse docking procedure, we expected to find a target with docking scores that would be maximal in the case of BOs with unsubstituted 1,4-benzoxazine moiety. To improve the sensitivity of the reverse docking procedure, we docked compounds from this paper together with the earlier reported anti-TB BOs.[8] For convenience, BOs from the study reported in Reference [8] are indicated with the same numbers as in the source paper, but marked with quotes (e.g., "2"). Compounds bearing a chiral atom were docked as both enantiomers (**6a** and **6a+**, **6b** and **6b+**).

Docking of BOs and their analogs to isocitrate lyase (*icl1*; Entry 23, Table 3) resulted in negative scores, which meant that ligands were much larger than the cavity of the binding site. Thus, this protein was not processed further.

Obtained docking scores were normalized and distributed in five categories to visualize ligand ranks to each protein (Figure 3). According to Figure 3, compounds most active in biological assays, BOs **1a,b,d,l,q**, had highest normalized docking scores (top 25%) only to aspartate 1-decarboxylase (*panD*; Entry 22, Table 3). Considering this, we assumed that a putative target of BO **1** in *Mtb* could be *panD*.

PanD catalyzes decarboxylation of L-aspartate to result in β-alanine and CO_2. This is a part of the pantothenate biosynthetic pathway.[20]

Pyrazinamide (PZA) is a clinically effective anti-TB drug. Recently, PZA's mechanism of action was investigated by Sun et al.[21]; *panD* was found to be concurrently inhibited by pyrazinoic acid (POA)[21] formed from PZA by the enzyme pyrazinamidase, *pncA* (*Rv2043c*).[22] So, the substrate of *panD* is L-aspartate and POA is its concurrent inhibitor. BO **1** contains an aspartate-like motif (Figure 4), which, apparently, determined good docking scores of BO **1** to *panD*.

Docking characteristics of BOs **1a,b,d,l,q** to cavity of *panD* are summarized in Table 4. For comparison, similar characteristics of POA (natural ligand of 6oyy, Figure 4) and 6-chloro-POA (natural ligand of 6p02, Figure 4) are provided.

Four hydrogen bonds (HBs) contribute significantly to the binding between POA and *panD*: with Ala74, Ala75, and two with Arg54.[21] In the best-docked poses of BOs **1a,b,d,l,q**, some of these significant HBs were observed along with some other HBs and other types of interactions (Figure 5). The best-docked pose of BO **1l** showed an unfavorable bump of an alkyloyl substituent with Tyr22. We suppose that this unfavorable interaction could be corrected by flexibility of this amino acid residue or flexibility of alkyloyl substituent in BO **1l**. The best-docked poses of other BOs **1a,b,d,q** had no unfavorable interactions.

Notably, docked BOs having a bulky substituent in 1,4-benzoxazine moiety suffered additional unfavorable interactions with the protein, which could explain the deterioration of anti-TB activity of such BOs in comparison with unsubstituted ones (protein–ligand interactions in the example of BO **1i** are shown in Figure 6).

Moreover, aza analog of BOs, quinoxalinone "12," reported to be inactive in anti-TB assays,[8] was found not to form significant HBs with Ala75 and Arg54 and to suffer an unfavorable interaction with Tyr22 (Figure 7), in comparison with its analog, BO **1a** (Figure 5b), active in anti-TB assay.[8] Similar SAR is known for PZA and POA.

TABLE 3 Targets of *Mtb* selected for reverse docking

Entry	PDB ID	Protein (gene)
1	4ohu, 4tzk, 5g0t	Enoyl-ACP reductase (*inhA*)
2	1uzn	β-Ketoacyl-ACP reductase (*mabA*)
3	5ld8, 6p9l, 6p9m	β-Ketoacyl-ACP synthase (*kasA*)
4	2gp6	β-Ketoacyl-ACP synthase (*kasB*)
5	2qo1	β-Ketoacyl-ACP synthase (*fabH*)
6	1 l1e	Cyclopropane synthase (*pcaA*)
7	1kpg, 1kph	Cyclopropane synthase (*cmaA1*)
8	1kpi	Cyclopropane synthase (*cmaA2*)
9	1tpy	Cyclopropane synthase (*mmaA2*)
10	6c4q	Polyketide synthase (*pks13*)
11	3ha5	*S*-Adenosylmethionine-dependent methyltransferase (*mmaA4*)
12	5hm3	Acyl-AMP ligase (*fadD32*)
13	4ewl	*N*-Acetyl-1-D-myo-inosityl-2-deoxy-α-D-glucopyranoside deacetylase (*mshB*)
14	1ozp, 1p0h	Mycothiol synthase (*mshD*)
15	4n9w, 4nc9	Phosphatidyl mannosyltransferase (*pimA*)
16	1q9j	Phthiocerol dimycocerosyl transferase (*papA5*)
17	5zue	Filamentation temperature-sensitive protein (*ftsZ*)
18	4qij	1,4-Dihydroxy-2-naphthoate-coenzyme A synthase (*menB*)
19	6o0j	2-Succinyl-5-enolpyruvyl-6-hydroxy-3-cyclohexene-1-carboxylate synthase (*menD*)
20	6ddp, 6nnh, 6nni	Dihydrofolate reductase (*dfrA*)
21	1mop, 1n2h, 4fzj	Pantothenate synthetase (*panC*)
22	6p02, 6oyy, 6oz8	Aspartate decarboxylase (*panD*)
23	5dql	Isocitrate lyase (*icl1*)
24	6ee1	Isocitrate lyase (*icl2*)
25	5ecv, 5h8u, 5t8g	Malate synthase (*glcB*)
26	5xnx	RelA protein (*relA*)
27	6c67	Adenosine kinase (*Rv2202c*)
28	4unr	Thymidylate kinase (*tmk*)
29	2a8x, 4m52	Dihydrolipoyl dehydrogenase (*lpdC*)
30	2isy	Iron-dependent regulator (*IdeR*)
31	1zlj	DosR regulator protein (*DosR*)
32	1z6k	Citrate lyase (*citE*)
33	4tvm	Citrate synthase (*gltA2*)
34	2byo	Lipoprotein LppX (*Rv2945c*)
35	5uhb	Transcription initiation complex (*Rv3457c*)

So, PZA itself does not inhibit *panD*, and its oxygen analog, POA, inhibits it (Figure 8).[21]

To evaluate the possibility of binding of BOs **1a,b,d,l,q** to mutant *panD* from PZA-resistant strains, we performed their docking to a *panD* available in PDB (6p1y). This mutant protein is characterized by a smaller volume of the active site.[21] Docking characteristics of BOs **1a,b,d,l,q** and POAs to cavity of mutant *panD* are summarized in Table 5. The best-docked poses of BOs **1a,b,d,l,q** to mutant *panD* had lower docking scores

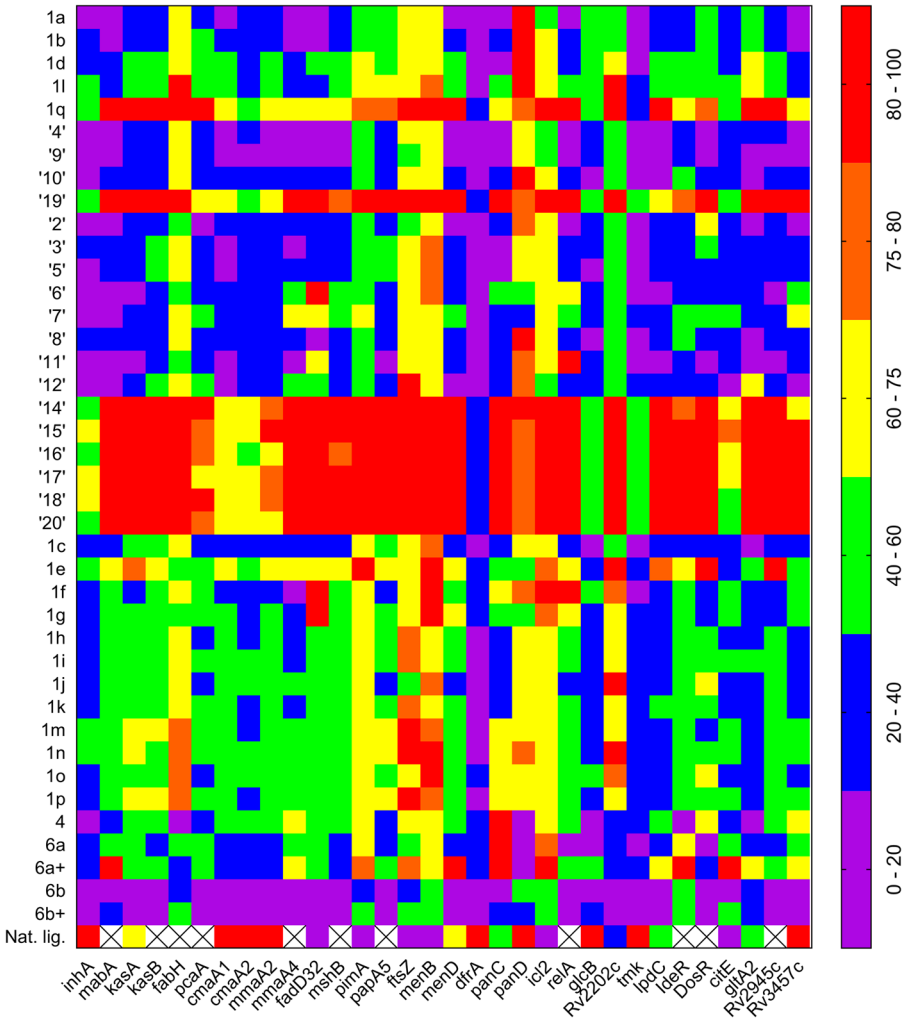

FIGURE 3 Categorized normalized docking scores

in comparison with docking to non-mutant *panD* and showed unfavorable interactions with the protein (Figure 9). So, we can conclude that BOs **1a,b,d,l,q** would be less active in nature to the mutant *panD* and would not affect such PZA-resistant strains. Nonetheless, most of the PZA clinical resistance cases are due to loss-of-function mutations in pyrazinamidase (*pncA*).[22] Considering this, if our hypothesis about the mechanism of action of BO **1** is true, it could be a useful drug for treatment of some cases of PZA-resistant TB.

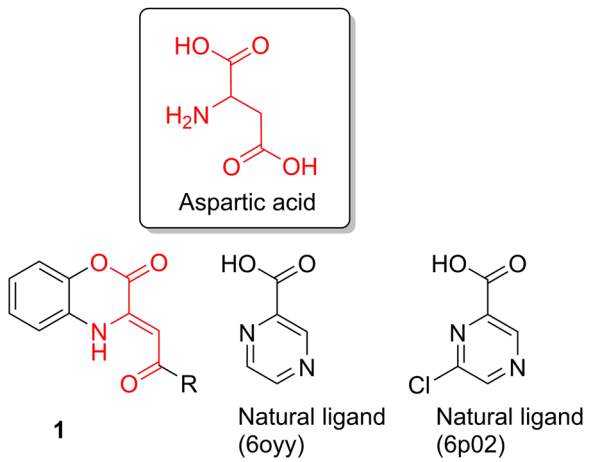

FIGURE 4 Aspartate-like motif in 1,4-benzoxazin-2-ones bearing the enaminone moiety **1** and pyrazinoic acid

TABLE 4 Docking scores and binding energies of BOs **1a,b,d,l,q** to cavity of *panD*

Ligand	Scores	ΔG_{bind} (kJ/mol)
1a	24.37[a]	−29.21
1b	23.08[a]	−30.64
1d	24.89[a]	−37.01
1l	25.79[a]	−37.06
1q	22.62[a]	−33.48
Natural ligand (6p02)	26.75[a]	−26.99
Natural ligand (6oyy)	24.82[b]	−25.17

Abbreviations: BO, 1,4-benzoxazin-2-ones bearing the enaminone moiety; *panD*, aspartate decarboxylase.
[a]Docked to 6p02.
[b]Docked to 6oyy.

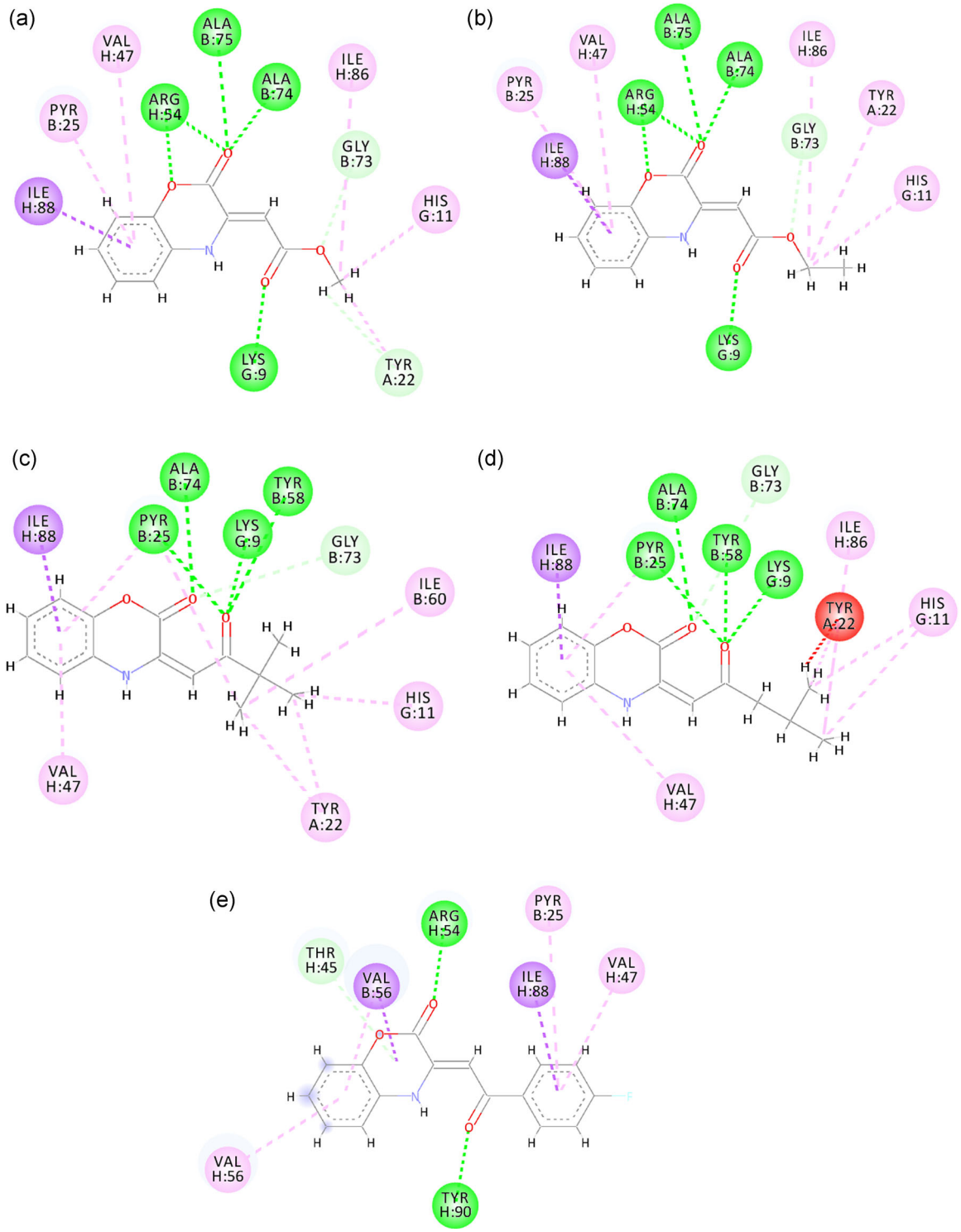

FIGURE 5 Protein–ligand interactions of 1,4-benzoxazin-2-ones bearing the enaminone moiety **1a** (a), **1b** (b), **1d** (c), **1l** (d), **1q** (e) with *panD* (6p02). Red, unfavorable bumps; green, conventional hydrogen bonds; pale green, carbon hydrogen bonds; pale pink, alkyl and π–alkyl interactions; violet: π–σ interactions

3 | CONCLUSION

We tested 17 BOs, their novel open-ring analogs, and two annelated analogs of BOs for in vitro antibacterial activity against *Mtb* (H37Rv). BOs bearing the unsubstituted 1,4-benzoxazin-2-one moiety showed the most promising activities (MBC = 5.00 µg/ml after 41 days of incubation). For the four most active compounds, the bacteriostatic activity was determined daily during the 41 days. The most promising compound **1d** showed a bacteriostatic effect at a concentration of 0.31 µg/ml on Day 4, 0.62 µg/ml on Day 6, 2.50 µg/ml on Day 9, and 5.00 µg/ml on Day 41.

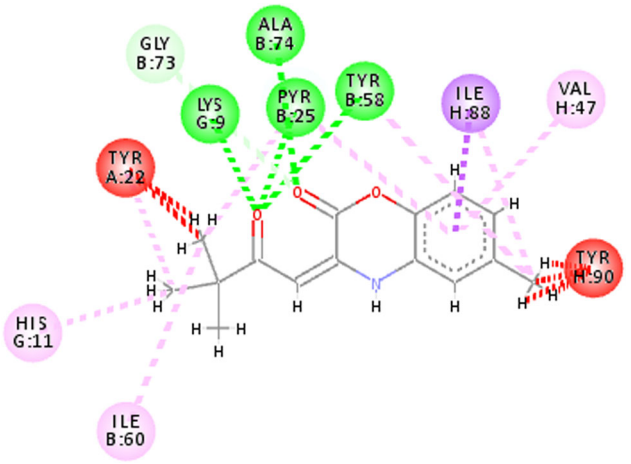

FIGURE 6 Protein–ligand interactions of 1,4-benzoxazin-2-ones bearing the enaminone moiety **1i** with *panD* (6p02). Red, unfavorable bumps; green, conventional hydrogen bonds (HBs); pale green, carbon HBs; pale pink, alkyl and π–alkyl interactions; violet, π–σ interactions

All studied compounds along with their reported analogs[8] were docked to 35 proteins of *Mtb* (H37Rv) to find their potent targets. In the result of reverse docking, aspartate 1-decarboxylase, *panD*, was selected as the most appropriate target. Docking of the most active compounds to mutant *panD* from PZA-resistant strains of *Mtb* implied that they would not be active against these strains. Considering that most of the PZA clinical resistance cases are due to loss-of-function mutations in pyrazinamidase, *pncA*, these compounds could be useful drugs for the treatment of some cases of pyrazinamide-resistant TB.

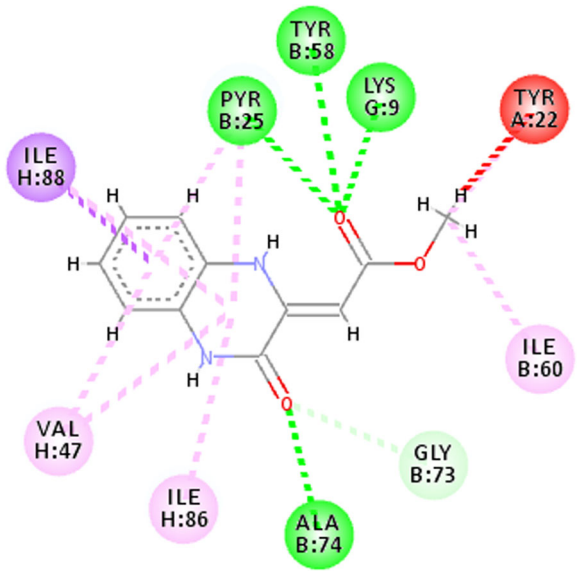

FIGURE 7 Protein–ligand interactions of quinoxalinone "12" with *panD* (6p02). Red, unfavorable bumps; green, conventional hydrogen bonds; pale green, carbon hydrogen bonds; pale pink, alkyl and π–alkyl interactions; violet, π–σ interactions

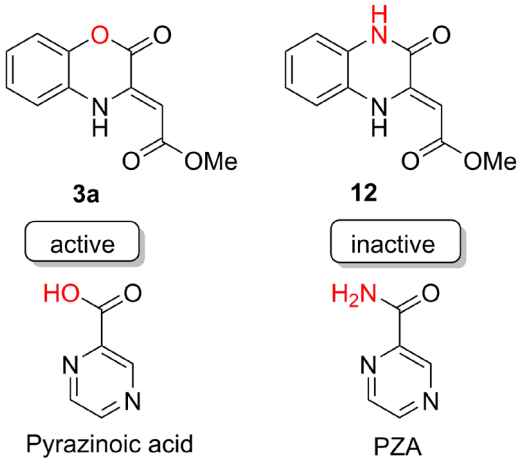

FIGURE 8 Comparison of pyrazinamide (PZA) and quinoxalinone "12" with their oxa analogs

4 | EXPERIMENTAL

4.1 | Chemistry

4.1.1 | General

^{1}H and ^{13}C NMR (nuclear magnetic resonance) spectra (see the Supporting Information) were acquired on a Bruker Avance-III spectrometer (400 and 100 MHz, respectively) in $CDCl_3$ or dimethyl sulfoxide (DMSO)-d_6 using hexamethyldisilazane or tetramethylsilane signals (in ^{1}H NMR) or solvent residual signals (in ^{1}H NMR, 7.27 for $CDCl_3$, 2.50 for DMSO-d_6; in ^{13}C NMR, 77.00 for $CDCl_3$, 39.51 for DMSO-d_6) as internal standards. Infrared (IR) spectra were recorded on a PerkinElmer Spectrum Two spectrometer from mulls in mineral oil. Melting points were measured on a Mettler Toledo MP70 apparatus. The single-crystal X-ray analysis was performed on an Xcalibur Ruby diffractometer. Elemental analyses were carried out on a Vario MICRO Cube analyzer. The purity of all compounds was examined using ultra-high pressure liquid chromatography (UPLC)-ultraviolet (UV)-mass spectrometry (MS); Waters ACQUITY UPLC I-Class system; Acquity UPLC BEH C18 column, grain size

TABLE 5 Docking scores and binding energies of 1,4-benzoxazin-2-ones bearing the enaminone moiety (BOs) **1a,b,d,l,q** to cavity of mutant *panD* (6p1y)

BO	Scores	ΔG_{bind} (kJ/mol)
1a	21.87	−27.91
1b	22.80	−27.14
1d	22.86	−34.50
1l	26.06	−34.50
1q	24.21	−40.29
Natural ligand (6p02)	26.15	−26.66
Natural ligand (6oyy)	24.63	−24.80

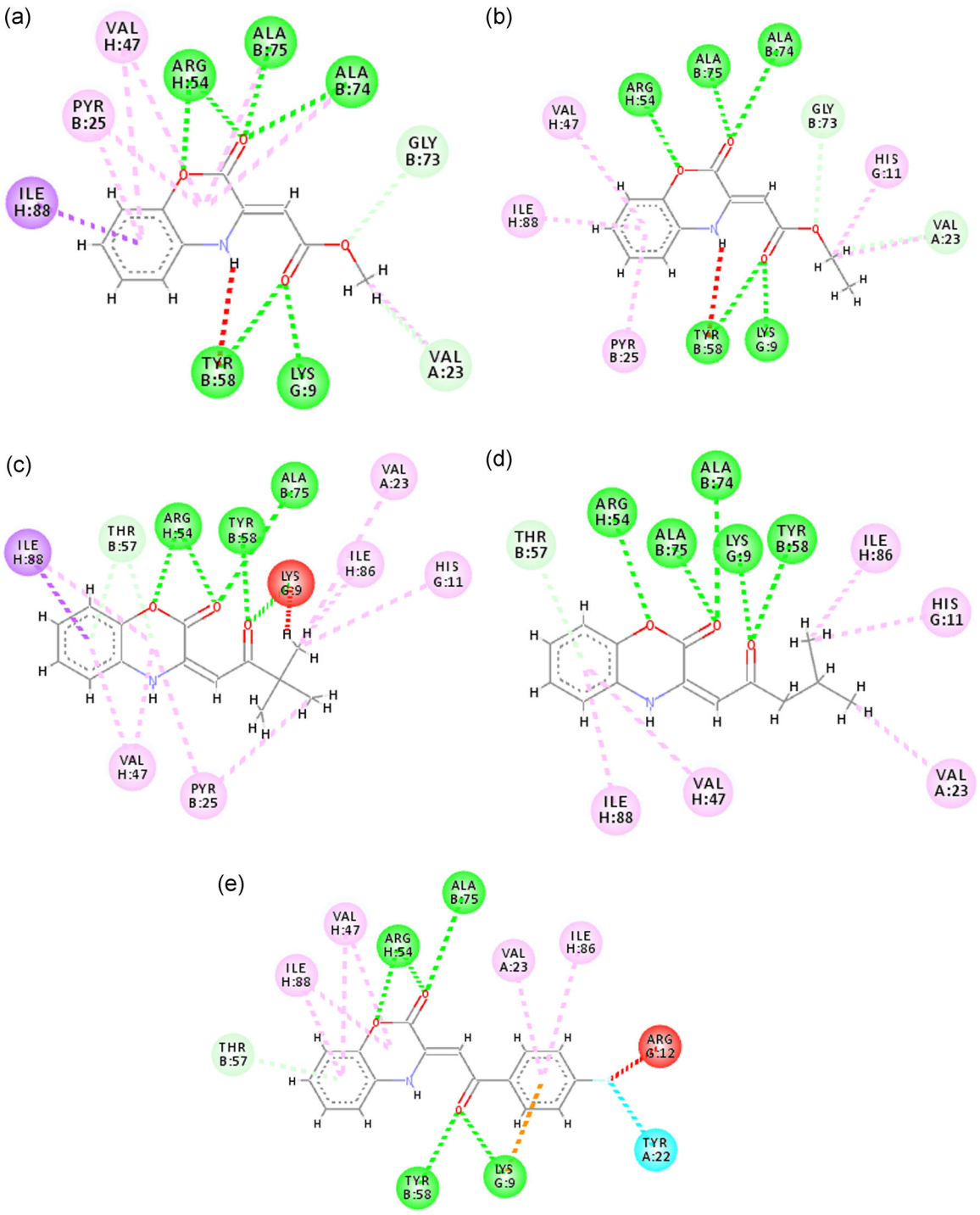

FIGURE 9 Protein–ligand interactions of 1,4-benzoxazin-2-ones bearing the enaminone moiety **1a** (a), **1b** (b), **1d** (c), **1l** (d), **1q** (e) with mutant *panD* (6p1y). Red, unfavorable interactions; green, conventional hydrogen bonds; pale green, carbon hydrogen bonds; pale pink, alkyl and π–alkyl interactions; violet, π–σ interactions; blue, halogen bonds (fluorine); orange, π–cation interactions

of 1.7 μm; acetonitrile–water as eluents; flow rate of 0.6 ml/min; ACQUITY UPLC PDA eλ detector (wavelength range of 230–780 nm; Xevo TQD mass detector; electrospray ionization (ESI); positive and negative ion detection; ion source temperature of 150°C; capillary voltage of 3.5–4.0 kV; cone voltage of 20–70 V; vaporizer temperature of 200°C.

Benzene and hexane were distilled over Na before the use. All other solvents and reagents were purchased from commercial vendors and were used as received.

The InChI codes of the investigated compounds, together with some biological activity data, are provided as Supporting Information.

4.1.2 | Procedure for the synthesis of BO 1a

DMAD (4.1 mmol, 0.5 ml) was added to a stirring suspension of *o*-aminophenol **2a** (4.1 mmol, 0.45 g) in methanol (5 ml). The reaction mixture was stirred at room temperature overnight. The formed yellow precipitate was filtered off, washed with methanol (15 ml), and recrystallized from ethanol (50 ml) to give BO **1a**.

*Methyl (2Z)-(2-oxo-2*H*-1,4-benzoxazin-3(4*H*)-ylidene)acetate (**1a**)*[9]
Yield: 0.68 g (76%); yellow solid; mp 163–165°C (ethanol; mp[9] 164–168°C). ^{1}H NMR (DMSO-d_6): δ = 10.66 (s, 1H), 7.50 (m, 1H), 7.18 (m, 2H), 7.04 (m, 1H), 5.64 (s, 1H), and 3.72 (s, 3H) ppm. IR: ν = 3,337, 1,768, 1,723, and 1,666 cm^{-1}. MS (ESI+): *m/z* calcd for $C_{11}H_9NO_4$+H$^+$: 220.06 [M+H]$^+$; found: 220.02. Anal. calcd (%) for $C_{11}H_9NO_4$: C 60.28; H 4.14; N 6.39. Found: C 60.12; H 4.16; N 6.41.

4.1.3 | General procedure for the synthesis of BOs 1b–q

Alkyl acylpyruvate **3a–d** (4.0 mmol) was added to a suspension of *o*-aminophenol **2a–h** (4.0 mmol) in ethanol (10 ml). The reaction mixture was refluxed for 5 min and cooled to ambient temperature. The formed yellow precipitate was filtered off, washed with ethanol (5 ml), and recrystallized to give BO **1b–q**.

*Ethyl (2Z)-(2-oxo-2*H*-1,4-benzoxazin-3(4*H*)-ylidene)acetate (**1b**)*[10]
Yield: 0.63 g (71%); yellow solid; mp 110–112°C (ethanol; mp[10] 116–117°C). ^{1}H NMR ($CDCl_3$): δ = 10.70 (s, 1H), 7.14 (m, 2H), 7.00 (m, 2H), 5.94 (s, 1H), 4.24 (q, *J* = 7.2 Hz, 2H), and 1.33 (t, *J* = 7.2 Hz, 3H) ppm. IR: ν = 3,214, 1,760, and 1,661 cm^{-1}. MS (ESI+): *m/z* calcd for $C_{12}H_{11}NO_4$+H$^+$: 234.08 [M+H]$^+$; found: 234.12. Anal. calcd (%) for $C_{12}H_{11}NO_4$: C 61.80; H 4.75; N 6.01. Found: C 61.98; H 4.76; N 6.01.

*Ethyl (2Z)-(6-bromo-2-oxo-2*H*-1,4-benzoxazin-3(4*H*)-ylidene)acetate (**1c**)*
Yield: 0.97 g (78%); yellow solid; mp 137–139°C (ethanol). ^{1}H NMR (DMSO-d_6): δ = 10.67 (s, 1H), 7.83 (m, 1H), 7.15 (m, 2H), 5.64 (s, 1H), 4.19 (q, *J* = 7.1 Hz, 2H), and 1.26 (t, *J* = 7.1 Hz, 3H) ppm. ^{13}C NMR (DMSO-d_6): δ = 167.7, 155.5, 139.1, 137.9, 126.2, 124.5, 118.3, 118.0, 116.5, 89.9, 59.6, and 14.1 ppm. IR: ν = 3,179, 1,771, and 1,668 cm^{-1}. MS (ESI+): *m/z* calcd for $C_{12}H_{10}BrNO_4$+H$^+$: 311.99, 313.99 [M+H]$^+$; found: 311.96, 313.96. Anal. calcd (%) for $C_{12}H_{10}BrNO_4$: C 46.18; H 3.23; N 4.49. Found: C 46.00; H 3.30; N 4.43.

*(3Z)-3-(3,3-Dimethyl-2-oxobutylidene)-3,4-dihydro-2*H*-1,4-benzoxazin-2-one (**1d**)*[14]
Yield: 0.81 g (83%); yellow solid; mp 86–88°C (ethanol; mp[14] 80–81°C). ^{1}H NMR (DMSO-d_6): δ = 12.33 (s, 1H), 7.48 (m, 1H), 7.19 (m, 2H), 7.08 (m, 1H), 6.36 (s, 1H), and 1.18 (s, 9H) ppm. ^{13}C NMR (DMSO-d_6): δ = 206.1, 156.0, 140.6, 138.6, 125.1, 124.0, 123.0, 116.3, 116.2, 92.1, 42.3, and 26.7 (3C) ppm. IR: ν = 3,180, 1,772, and 1,632 cm^{-1}. MS (ESI+): *m/z* calcd for $C_{14}H_{15}NO_3$+H$^+$: 246.11 [M+H]$^+$; found: 246.12. Anal. calcd (%) for $C_{14}H_{15}NO_3$: C 68.56; H 6.16; N 5.71. Found: C 68.41; H 6.16; N 5.76. The complete set of X-ray diffraction data was deposited to the Cambridge Crystallographic Data Centre (CCDC; Entry no. 2005170); it can be requested at www.ccdc.cam.ac.uk.

*(2Z)-2-(3,3-Dimethyl-2-oxobutylidene)-1,2-dihydro-3*H*-naphtho-[2,1-b][1,4]oxazin-3-one (**1e**)*
1-Aminonaphthalen-2-ol **2h** hydrochloride was utilized in general procedure instead of 1-aminonaphthalen-2-ol **2h**. Yield: 0.74 g (63%); yellow solid; mp 168–169°C (ethanol). ^{1}H NMR (DMSO-d_6): δ = 13.75 (s, 1H), 7.98 (m, 1H), 7.87 (m, 1H), 7.73 (m, 2H), 7.59 (m, 1H), 7.41 (m, 1H), 6.44 (s, 1H), and 1.24 (s, 9H) ppm. ^{13}C NMR (DMSO-d_6): δ = 206.7, 155.7, 139.7, 138.0, 130.3, 128.7, 127.6, 126.1, 123.7, 120.9, 118.8, 117.5, 116.3, 91.9, 42.3, and 26.9 (3C) ppm. IR: ν = 3,177, 1,758, and 1,631 cm^{-1}. MS (ESI+): *m/z* calcd for $C_{18}H_{17}NO_3$+H$^+$: 296.13 [M+H]$^+$; found: 296.13. Anal. calcd (%) for $C_{18}H_{17}NO_3$: C 73.20; H 5.80; N 4.74. Found: C 73.41; H 5.68; N 4.75.

*(3Z)-3-(3,3-Dimethyl-2-oxobutylidene)-7-nitro-3,4-dihydro-2*H*-1,4-benzoxazin-2-one (**1f**)*
Yield: 0.82 g (71%); yellow solid; mp 201–202°C (ethanol). ^{1}H NMR (DMSO-d_6): δ = 12.22 (s, 1H), 8.04 (m, 2H), 7.75 (m, 1H), 6.50 (s, 1H), and 1.19 (s, 9H) ppm. ^{13}C NMR (DMSO-d_6): δ = 206.6, 155.4, 141.4, 140.1, 137.3, 130.8, 120.8, 116.4, 111.9, 95.2, 42.8, and 26.4 (3C) ppm. IR: ν = 3,182, 1,768, and 1,646 cm^{-1}. MS (ESI+): *m/z* calcd for $C_{14}H_{14}N_2O_5$+H$^+$: 291.10 [M+H]$^+$; found: 291.12. Anal. calcd (%) for $C_{14}H_{14}N_2O_5$: C 57.93; H 4.86; N 9.65. Found: C 58.12; H 4.80; N 9.63.

*(3Z)-3-(3,3-Dimethyl-2-oxobutylidene)-6-nitro-3,4-dihydro-2*H*-1,4-benzoxazin-2-one (**1g**)*
Yield: 0.84 g (73%); yellow solid; mp 194–195°C (ethanol). ^{1}H NMR (DMSO-d_6): δ = 12.19 (s, 1H), 8.63 (m, 1H), 7.89 (m, 1H), 7.40 (m, 1H), 6.43 (s, 1H), and 1.19 (s, 9H) ppm. ^{13}C NMR (DMSO-d_6): δ = 206.0, 155.5, 145.0, 144.1, 137.6, 125.4, 117.7, 117.0, 112.0, 93.9, 42.5, and 26.5 (3C) ppm. IR: ν = 3,194, 1,768, and 1,633 cm^{-1}. MS (ESI+): *m/z* calcd for $C_{14}H_{14}N_2O_5$+H$^+$: 291.10 [M+H]$^+$; found: 291.10. Anal. calcd (%) for $C_{14}H_{14}N_2O_5$: C 57.93; H 4.86; N 9.65. Found: C 58.19; H 4.89; N 9.64.

*(3Z)-6-Bromo-3-(3,3-dimethyl-2-oxobutylidene)-3,4-dihydro-2*H*-1,4-benzoxazin-2-one (**1h**)*
Yield: 0.95 g (73%); yellow solid; mp 153–154°C (ethanol). ^{1}H NMR (DMSO-d_6): δ = 12.14 (s, 1H), 7.85 (m, 1H), 7.18 (m, 2H), 6.38 (s, 1H), and 1.18 (s, 9H) ppm. ^{13}C NMR (DMSO-d_6): δ = 206.1, 155.8, 139.9, 138.0, 125.8, 125.2, 118.8, 118.0, 116.5, 93.2, 42.4, and 26.6 (3C) ppm. IR: ν = 3,177, 1,765, and 1,633 cm^{-1}. MS (ESI+): *m/z* calcd for $C_{14}H_{14}BrNO_3$+H$^+$: 324.02, 326.02 [M+H]$^+$; found: 324.04, 326.04. Anal. calcd (%) for $C_{14}H_{14}BrNO_3$: C 51.87; H 4.35; N 4.32. Found: C 52.03; H 4.33; N 4.12.

*(3Z)-3-(3,3-Dimethyl-2-oxobutylidene)-6-methyl-3,4-dihydro-2*H*-1,4-benzoxazin-2-one (**1i**)*
Yield: 0.84 g (81%); yellow solid; mp 142–143°C (ethanol). ^{1}H NMR (DMSO-d_6): δ = 12.31 (s, 1H), 7.26 (m, 1H), 7.08 (m, 1H), 6.89 (m, 1H),

6.34 (s, 1H), 2.28 (s, 3H), and 1.17 (s, 9H) ppm. ^{13}C NMR (DMSO-d_6): δ = 206.1, 156.1, 138.7, 134.6, 123.7, 123.5, 116.3, 115.9, 92.1, 42.3, 26.7 (3C), and 20.3 ppm. IR: ν = 3,161, 1,771, and 1,636 cm^{-1}. MS (ESI+): *m/z* calcd for $C_{15}H_{17}NO_3$+H$^+$: 260.13 [M+H]$^+$; found: 260.18. Anal. calcd (%) for $C_{15}H_{17}NO_3$: C 69.48; H 6.61; N 5.50. Found: C 69.21; H 6.60; N 5.53.

*(3Z)-3-(3,3-Dimethyl-2-oxobutylidene)-5-methyl-3,4-dihydro-2H-1,4-benzoxazin-2-one (**1j**)*

Yield: 0.86 g (83%); yellow solid; mp 121–122°C (ethanol). ^{1}H NMR (DMSO-d_6): δ = 12.77 (s, 1H), 7.06 (m, 3H), 6.39 (s, 1H), 2.34 (s, 3H), and 1.19 (s, 9H) ppm. ^{13}C NMR (DMSO-d_6): δ = 207.0, 155.7, 140.9, 139.2, 126.3, 123.5, 122.8, 122.1, 114.2, 92.0, 42.4, 26.8 (3C), and 15.6 ppm. IR: ν = 3,172, 1,771, 1,756, and 1,631 cm^{-1}. MS (ESI+): *m/z* calcd for $C_{15}H_{17}NO_3$+H$^+$: 260.13 [M+H]$^+$; found: 260.17. Anal. calcd (%) for $C_{15}H_{17}NO_3$: C 69.48; H 6.61; N 5.50. Found: C 69.27; H 6.57; N 5.54.

*(3Z)-6-Chloro-3-(3,3-dimethyl-2-oxobutylidene)-3,4-dihydro-2H-1,4-benzoxazin-2-one (**1k**)*

Yield: 0.85 g (76%); yellow solid; mp 149–150°C (ethanol). ^{1}H NMR (DMSO-d_6): δ = 12.15 (s, 1H), 7.72 (m, 1H), 7.21 (m, 1H), 7.07 (m, 1H), 6.39 (s, 1H), and 1.18 (s, 9H) ppm. ^{13}C NMR (DMSO-d_6): δ = 206.1, 155.8, 139.5, 138.0, 128.7, 125.5, 122.3, 117.6, 115.9, 93.2, 42.4, and 26.6 (3C) ppm. IR: ν = 3,177, 1,763, and 1,636 cm^{-1}. MS (ESI+): *m/z* calcd for $C_{14}H_{14}ClNO_3$+H$^+$: 280.07 [M+H]$^+$; found: 280.09. Anal. calcd (%) for $C_{14}H_{14}ClNO_3$: C 60.12; H 5.05; N 5.01. Found: C 60.32; H 5.01; N 5.22.

*(3Z)-3-(4-Methyl-2-oxopentylidene)-3,4-dihydro-2H-1,4-benzoxazin-2-one **(1l)***

Yield: 0.77 g (79%); yellow solid; mp 108–110°C (ethanol). ^{1}H NMR (DMSO-d_6): δ = 12.25 (s, 1H), 7.48 (m, 1H), 7.19 (m, 2H), 7.08 (m, 1H), 6.14 (s, 1H), 2.40 (d, *J* = 7.1 Hz, 2H), 2.09 (m, 1H), and 0.93 (d, *J* = 6.8 Hz, 6H) ppm. ^{13}C NMR (DMSO-d_6): δ = 200.7, 155.9, 140.7, 137.4, 125.1, 124.0, 123.0, 116.2, 116.2, 96.8, 51.4, 25.2, and 22.3 (2C) ppm. IR: ν = 3,177, 1,758, and 1,641 cm^{-1}. MS (ESI+): *m/z* calcd for $C_{14}H_{15}NO_3$+H$^+$: 246.11 [M+H]$^+$; found: 246.13. Anal. calcd (%) for $C_{14}H_{15}NO_3$: C 68.56; H 6.16; N 5.71. Found: C 68.79; H 6.06; N 5.77.

*(3Z)-6-Chloro-3-(4-methyl-2-oxopentylidene)-3,4-dihydro-2H-1,4-benzoxazin-2-one (**1m**)*

Yield: 0.84 g (75%); yellow solid; mp 135–136°C (ethanol). ^{1}H NMR (DMSO-d_6): δ = 12.07 (s, 1H), 7.71 (m, 1H), 7.21 (m, 1H), 7.07 (m, 1H), 6.17 (s, 1H), 2.41 (d, *J* = 6.8 Hz, 2H), 2.10 (m, 1H), and 0.93 (d, *J* = 6.6 Hz, 6H) ppm. ^{13}C NMR (DMSO-d_6): δ = 200.8, 155.7, 139.5, 136.6, 128.7, 125.5, 122.3, 117.6, 115.9, 97.8, 51.5, 25.1, and 22.3 (2C) ppm. IR: ν = 3,204, 1,763, and 1,648 cm^{-1}. MS (ESI+): *m/z* calcd for $C_{14}H_{14}ClNO_3$+H$^+$: 280.07 [M+H]$^+$; found: 280.08. Anal. calcd (%) for $C_{14}H_{14}ClNO_3$: C 60.12; H 5.05; N 5.01. Found: C 60.24; H 5.12; N 5.03.

*(3Z)-6-Methyl-3-(4-methyl-2-oxopentylidene)-3,4-dihydro-2H-1,4-benzoxazin-2-one (**1n**)*

Yield: 0.81 g (73%); yellow solid; mp 89–90°C (ethanol). ^{1}H NMR (DMSO-d_6): δ = 12.25 (s, 1 H), 7.26 (m, 1H), 7.09 (m, 1H), 6.89 (m, 1H), 6.13 (s, 1H), 2.39 (d, *J* = 7.1 Hz, 2H), 2.28 (s, 3H), 2.09 (m, 1H), and 0.92 (d, *J* = 6.6 Hz, 6H) ppm. ^{13}C NMR (DMSO-d_6): δ = 200.7, 156.0, 138.7, 137.4, 134.7, 123.6, 123.5, 116.3, 115.9, 96.7, 51.4, 25.3, 22.3 (2C), and 20.3 ppm. IR: ν = 3,189, 1,768, 1,758, and 1,641 cm^{-1}. MS (ESI+): *m/z* calcd for $C_{15}H_{17}NO_3$+H$^+$: 260.13 [M+H]$^+$; found: 260.15. Anal. calcd (%) for $C_{15}H_{17}NO_3$: C 69.48; H 6.61; N 5.50. Found: C 69.34; H 6.67; N 5.53.

*(3Z)-5-Methyl-3-(4-methyl-2-oxopentylidene)-3,4-dihydro-2H-1,4-benzoxazin-2-one (**1o**)*

Yield: 0.85 g (76%); yellow solid; mp 99°C (ethanol). ^{1}H NMR (DMSO-d_6): δ = 12.76 (s, 1H), 7.11 (m, 2H), 7.03 (m, 1H), 6.19 (s, 1H), 2.42 (d, *J* = 7.1 Hz, 2H), 2.34 (s, 3H), 2.11 (m, 1H), and 0.93 (d, *J* = 6.8 Hz, 6H) ppm. ^{13}C NMR (DMSO-d_6): δ = 201.6, 155.6, 141.0, 138.1, 126.3, 123.5, 122.8, 122.2, 114.2, 96.6, 51.3, 25.4, 22.3 (2C), and 15.6 ppm. IR: ν = 3,167, 1,768, and 1,633 cm^{-1}. MS (ESI+): *m/z* calcd for $C_{15}H_{17}NO_3$+H$^+$: 260.13 [M+H]$^+$; found: 260.14. Anal. calcd (%) for $C_{15}H_{17}NO_3$: C 69.48; H 6.61; N 5.50. Found: C 69.69; H 6.63; N 5.47.

*(3Z)-6-Bromo-3-(4-methyl-2-oxopentylidene)-3,4-dihydro-2H-1,4-benzoxazin-2-one (**1p**)*

Yield: 0.92 g (71%); yellow solid; mp 130–131°C (ethanol). ^{1}H NMR (DMSO-d_6): δ = 12.06 (s, 1H), 7.84 (m, 1H), 7.17 (m, 2H), 6.17 (s, 1H), 2.41 (d, *J* = 7.1 Hz, 2H), 2.09 (m, 1H), and 0.93 (d, *J* = 6.6 Hz, 6H) ppm. ^{13}C NMR (DMSO-d_6): δ = 200.8, 155.7, 140.0, 136.6, 125.9, 125.2, 118.7, 118.0, 116.5, 97.8, 51.5, 25.2, and 22.3 (2C) ppm. IR: ν = 3,192, 1,766, and 1,646 cm^{-1}. MS (ESI+): *m/z* calcd for $C_{14}H_{14}BrNO_3$+H$^+$: 324.02, 326.02 [M+H]$^+$; found: 324.03, 326.03. Anal. calcd (%) for $C_{14}H_{14}BrNO_3$: C 51.87; H 4.35; N 4.32. Found: C 51.99; H 4.23; N 4.32.

*(3Z)-3-[2-(4-Fluorophenyl)-2-oxoethylidene]-3,4-dihydro-2H-1,4-benzoxazin-2-one (**1q**)*[23]

Yield: 0.90 g (80%); yellow solid; mp 186–187°C (toluene; mp[23] 190–192°C). ^{1}H NMR (DMSO-d_6): δ = 12.78 (s, 1H), 8.10 (m, 2H), 7.59 (m, 1H), 7.35 (m, 2H), 7.24 (m, 2H), 7.14 (m, 1H), and 6.87 (s, 1H) ppm. ^{13}C NMR (DMSO-d_6): δ = 188.0, 165.8, 163.3, 155.8, 141.1, 139.9, 134.7 (2C), 130.0, 129.9, 125.2, 123.8, 123.6, 116.7, 116.3, 115.8, 115.6, and 92.4 ppm. IR: ν = 3,100, 1,752, and 1,622 cm^{-1}. MS (ESI+): *m/z* calcd for $C_{16}H_{10}FNO_3$+H$^+$: 284.07 [M+H]$^+$; found: 284.05. Anal. calcd (%) for $C_{16}H_{10}FNO_3$: C 67.84; H 3.56; N 4.94. Found: C 68.02; H 3.55; N 4.89.

4.1.4 | Procedure for the synthesis of the open-ring analog of BO (4)

Diethyl oxaloacetate **3d** (4.0 mmol, 0.75 g) was added to a suspension of *N*-(2-aminophenyl)acetamide (4.0 mmol, 0.6 g) in ethanol (10 ml). The reaction mixture was refluxed for 5 min and then cooled to ambient temperature. The formed yellow precipitate was filtered off, washed with ethanol (5 ml), and recrystallized from ethanol (10 ml) to give compound **4**.

Diethyl 2-(2-acetamidoanilino)but-2-enedioate (4)

Yield: 0.85 g (66%); yellow solid; mp 99–101°C (ethanol). ^{1}H NMR (DMSO-d_6): δ = 9.88 (s, 1H), 9.40 (s, 1H), 7.26 (m, 1H), 7.13 (m, 2H), 6.81 (m, 1H), 5.22 (s, 1H), 4.12 (q, J = 7.1 Hz, 2H), 4.01 (q, J = 7.1 Hz, 2H), 2.08 (s, 3H), 1.23 (t, J = 7.1 Hz, 3H), and 0.96 (t, J = 7.1 Hz, 3H) ppm. ^{13}C NMR (DMSO-d_6): δ = 168.7, 167.4, 163.8, 148.0, 135.1, 130.6, 125.7, 125.1, 124.8, 122.6, 93.4, 61.5, 59.3. 22.8, 14.1, and 13.2 ppm. IR: ν = 3,184, 1,741, 1,686, and 1,663 cm^{-1}. MS (ESI+): *m/z* calcd for $C_{16}H_{20}N_2O_5$+H$^+$: 321.15 [M+H]$^+$; found: 321.19. Anal. calcd (%) for $C_{16}H_{20}N_2O_5$: C 59.99; H 6.29; N 8.74. Found: C 60.21; H 6.19; N 8.92.

4.1.5 | Procedures for the syntheses of the annelated analogs of BOs (5a,b)

Oxalyl chloride (6 mmol, 0.5 ml) was added to a suspension of BO **1q** (4 mmol, 1.1 g) in 20 ml of benzene. The reaction mixture refluxed for 110 min (gaseous HCl evolved) and then cooled to ambient temperature. The formed dark violet solid of compound **5a** was filtered off.

Oxalyl chloride (6 mmol, 0.5 ml) was added to a suspension of BO **1b** (4 mmol, 1.1 g) in 10 ml of benzene. The reaction mixture refluxed for 110 min (gaseous HCl evolved) and then cooled to ambient temperature. The solvent was removed under vacuum. The resulting dark violet solid of compound **5b** was grinded with hexane.

*3-(4-Fluorobenzoyl)-1*H*-pyrrolo[2,1-*c*][1,4]benzoxazine-1,2,4-trione (**5a**)*[23]

Yield: 1.22 g (91%); dark violet solid; mp 212–214°C (decomp., benzene; mp[23] 214–216°C). ^{1}H NMR (DMSO-d_6): δ = 8.38 (m, 1H), 8.22 (m, 2H), and 7.35 (m, 5H) ppm. MS (ESI+): *m/z* calcd for $C_{18}H_8FNO_5$+H_2O+H$^+$: 356.06 [M+H_2O+H]$^+$; found: 356.10. Anal. calcd (%) for $C_{18}H_8FNO_5$: C 64.10; H 2.39; N 4.15. Found: C 64.12; H 2.44; N 4.32.

*Ethyl 1,2,4-trioxo-2,4-dihydro-1*H*-pyrrolo[2,1-*c*][1,4]benzoxazine-3-carboxylate (**5b**)*[24]

Yield: 0.84 g (73%); dark violet solid; mp 156°C (decomp., hexane; mp[24] 156–157°C). ^{1}H NMR ($CDCl_3$): δ = 7.21–7.34 (m, 4H), 4.42 (m, 2H), and 1.39 (m, 3H) ppm. MS (ESI+): *m/z* calcd for $C_{14}H_9NO_6$+H_2O +H$^+$: 306.06 [M+H_2O+H]$^+$; found: 306.02. Anal. calcd (%) for $C_{14}H_9NO_6$: C 58.54; H 3.16; N 4.88. Found: C 58.34; H 2.91; N 4.81.

4.2 | Pharmacological/biological assays

4.2.1 | Bactericidal activity by BACTEC

The bactericidal activity of chemical compounds against *Mtb* (H37Rv) was studied by a standard BACTEC MGIT 960 radiometric growth system (Becton Dickinson).

Initial stock solutions of test compounds (10 mg/ml) were prepared in DMSO. Then, they were diluted with Middlebrook 7H9 sterile nutrient broth (9 ml) to result in the concentration of test compounds of 1,000 μg/ml. The aliquots of obtained solutions were treated by twofold serial dilutions and added to mycobacteria growth indicator tubes (MGITs) in quantities that provide the final concentrations (μg/ml): 20.0, 10.0, 5.0, 2.5, 1.25, 0.6, and 0.31. Each MGIT tube contained 7 ml of Middlebrook 7H9 sterile nutrient broth. Then, 0.8 ml of BACTEC MGIT OADC (oleic acid, albumin, dextrose, and catalase) growth supplement was added to each tube. In addition to the liquid medium, the tubes contained an oxygen-free fluorochrome, *tris*-4,7-diphenyl-1,10-phenanthroline ruthenium chloride pentahydrate (Ru[dpp]), placed at the bottom of the tube and coated with silicone.

A 1.0-McFarland suspension of *Mtb* (5×10^8 microbial cells per 1 ml) was prepared using a densitometer. Next, a solution was prepared by diluting the initial suspension 10 times with a sterile physiological saline solution, thus resulting in 5×10^7 microbial cells per 1 ml. Then, a suspension of *Mtb* (0.5 ml) was added to each of the above-prepared MGITs. In parallel, the inoculum of *Mtb* was loaded into control MGITs with Middlebrook 7H9 broth (0.5 ml), each containing no test compounds. For control, similar experiments were carried out with isoniazid (isonicotinic acid hydrazide, 99%; Sigma-Aldrich).

All tubes were incubated at 37°C and analyzed by BACTEC MGIT 960. If the compound is active against *Mtb*, it inhibits its growth and suppresses fluorescence of Ru(dpp), whereas, in the control tube, growth is not inhibited and, accordingly, the level of fluorescence in this tube is pronounced. During bacterial growth, free oxygen is consumed inside the tubes and replaced with CO_2. As free oxygen is consumed, inhibition of the fluorochrome, Ru(dpp), is stopped. Fluorescence becomes detectable when the test tube is irradiated with UV light and is automatically registered by photosensors of BACTEC MGIT 960. The minimum dilution of the examined compound, in which the growth was not registered by BACTEC, was taken as MBC. All assays were carried out in duplicate.

4.2.2 | Tuberculostatic activity by REMA

A 1.0-McFarland suspension of *Mtb* (H37Rv) was prepared and 0.1 ml was added to each of the following bottles: A direct control (bottle containing diluent, DMSO, but no test compound), a control containing a 1:100 organism dilution (also without test compound), and each concentration with the test compound.

From a culture of *Mtb*, which was in a log phase of growth in the Löwenstein–Jensen nutrient medium, a 1.0-McFarland suspension was prepared with a sterile physiological saline solution and 0.2% solution of Tween 80. The resulting suspension (50 μl) was transferred into a tube with 7H9 broth and OADC additive to give *Mtb* concentration of 1.5×10^6 CFU/ml.

Initial stock solutions (1,000 μg/ml) and subsequent dilutions of test compounds were prepared in DMSO. Further dilutions were performed by twofold dilutions of the stock solution with pure DMSO, that is, solutions with concentrations of 500, 250, 125, 62.5, 31.25, 15.63, and 7.81 μg/ml were obtained. The resulting solutions of the studied compounds (3.1 μl) were loaded into the wells of a 96-well plate, with each containing a culture medium (97 μl). Then, a suspension of *Mtb* (100 μl),

prepared as described above, was added to all wells of the plate. Final concentrations of test compounds in wells of a 96-well plate were 15.6, 7.8, 3.9, 1.95, 0.97, 0.49, 0.24, and 0.12 μg/ml; the final concentration of DMSO in wells was 1.6%. An *Mtb* culture without addition of compounds (100 μl of pure medium + 100 μl of a suspension of *Mtb*) and a culture of *Mtb* with DMSO (97 μl of a pure medium + 3.1 μl of DMSO + 100 μl of a suspension of *Mtb*) were used as a positive control. For control, similar experiments were carried out with isoniazid (initial stock solution and subsequent dilutions of isoniazid were prepared in water; final concentrations in wells of a 96-well plate were 0.007, 0.015, 0.031, 0.063, 0.125, 0.25, and 0.5 μg/ml).

The plates were incubated at 37°C for 7 days. Then, 50 μl of a resazurin (7-hydroxy-3*H*-phenoxazin-3-one 10-oxide) solution (with the addition of Tween 80) was added to the wells and the incubation was continued at 37°C. The results were monitored after 24, 48, and 72 hr. The minimum dilution of the examined compound in which there was no change in the blue-violet color of resazurin in all replicates was taken as MIC. All assays were carried out in triplicate.

4.3 | Molecular docking

4.3.1 | Ligands preparation

Two-dimensional structures of ligands were generated using the ChemDraw panel in ChemBio3D Ultra 14.0. 3D structures of ligands were generated by ChemBio3D Ultra 14.0. Energy minimization of ligand structures was performed by «MM2 minimize» function implemented in ChemBio3D Ultra 14.0. The SYBYL2 (*.mol2) format of structures was saved and used for docking study. In each structure bearing BO motif, serial numbers of atoms corresponding to the motif were set manually in ChemBio3D Ultra 14.0 to match each other in each structure.

4.3.2 | Proteins preparation

The crystal structures of proteins were downloaded from the Protein Data Bank (PDB; www.rcsb.org). Proteins preparation for docking was performed using the GOLD Docking Wizard in GOLD suit (2020.0 CSD Release). The proteins' preparation included the addition of hydrogen atoms, deletion of water molecules, and deletion of ligands (except for cofactors). For proteins available at PDB as several separate structures, two or three different structures were downloaded and superimposed at A-chains in GOLD Docking Wizard to best match weighting of 10.0 to consider protein flexibility.

Before docking to 6p1y, a tetramer of 6p1y was prepared by superimposition with chains of each subunit of a 6p02 tetramer in Hermes, the 3D visualizer provided with the CSD-Discovery Suite (2020.0 CSD Release), to best match weighting of 1.0. All waters and ligands in 6p1y were deleted and the resulting 6p1y structures were saved separately as *.pdb files in Hermes. The resulting *.pdb files were combined in Notepad for Windows 10 and saved as a single *.pdb file, which was re-saved in Hermes to afford the *.pdb file that was used for docking.

4.3.3 | Docking procedure

Ligand–protein docking was performed in GOLD suit (2020.0 CSD Release).

For protein structures having a native ligand (substrate or inhibitor), the binding site was determined as a space within a radius of 10–20 Å from the cavity of the deleted native ligand. For protein structures without a native ligand, the binding site was predicted by the comparison of docking solutions of ligand **3a** in the whole protein; the place where the ligand was most often located was considered as a binding site, and the final docking procedure for all examined ligands was performed in the space within a radius of 14–17 Å from a selected solvent-accessible atom from the predicted cavity for ligand **3a**.

Ligands were set as flexible with rotatable bonds. For ligands bearing the BO motif, rotatable bonds were overridden to make enaminone pattern flat and rigid (it was necessary to take into account the fact that BOs exist as enamino tautomers with *Z*-configuration of the exocyclic C=C, which is stabilized by the intramolecular chelate-type HB). Proteins were treated as rigid. For superimposed proteins, ensemble docking was applied to consider possible protein flexibility. ChemScore was used as a fitness function. If the top three solutions were within 1 Å, the number of genetic algorithm runs was terminated early. All other parameters and options in GOLD were used as default.

All calculations were carried out in triplicate. Statistical treatment was carried out using GraphPad Prism 8 (8.0.1 release) program. Best docking poses for each ligand were saved as *.pdb files in Hermes. Then protein–ligand interactions were determined by BIOVIA Discovery Studio Visualizer (Discovery Studio 2020 v20.1.0.19295) using default parameters and options.

ACKNOWLEDGMENTS

This study was supported by the Ministry of Science and Higher Education of the Russian Federation (FSNF-2020-0008) and the Government of Perm Krai. The authors thank the Ural Research Institute of Phthisiopulmonology (Yekaterinburg, Russia) for performing biological studies in vitro by REMA and Clinical Phthisiopulmonological Medical Center (Krasnokamsk, Russia) for performing biological studies in vitro by BACTEC.

CONFLICTS OF INTERESTS

The authors declare that there are no conflicts of interest.

ORCID

Ekaterina E. Stepanova http://orcid.org/0000-0002-5851-3082

REFERENCES

[1] E. S. Zuniga, J. Early, T. Parish, *Future Microbiol.* **2015**, *10*, 217. https://doi.org/10.2217/FMB.14.125

[2] V. Sharma, P. K. Jaiswal, D. K. Yadav, M. Saran, J. Prikhodko, M. Mathur, A. K. Swami, I. V. Mashevskaya, S. Chaudhary, *Acta Chim. Slov.* **2017**, *64*, 988. https://doi.org/10.17344/acsi.2017.3709

[3] R. Sharma, L. Yadav, J. Lal, P. K. Jaiswal, M. Mathur, A. K. Swami, S. Chaudhary, *Bioorg. Med. Chem. Lett.* **2017**, *27*, 4393. https://doi.org/10.1016/j.bmcl.2017.08.017

[4] I. V. Mashevskaya, I. A. Tolmacheva, E. V. Voronova, T. F. Odegova, G. A. Aleksandrova, A. F. Goleneva, S. V. Kol'tsova, A. N. Maslivets, *Pharm. Chem. J.* **2002**, *36*, 86. https://doi.org/10.1023/A:1016064014955
[5] P. P. Mukovoz, P. A. Slepukhin, E. A. Danilov, O. P. Aysuvakova, A. P. Glinushkin, *Russ. J. Gen. Chem.* **2018**, *88*, 1363. https://doi.org/10.1134/S1070363218070022
[6] X. Dou, H. Huang, Y. Li, L. Jiang, Y. Wang, H. Jin, N. Jiao, L. Zhang, L. Zhang, Zh Liu, *J. Med. Chem.* **2019**, *62*, 6645. https://doi.org/10.1021/acs.jmedchem.9b00537
[7] P. K. Jaiswal, V. Sharma, S. Kumar, M. Mathur, A. K. Swami, D. K. Yadav, S. Chaudhary, *Arch. Pharm.* **2018**, *351*, e1700349. https://doi.org/10.1002/ardp.201700349
[8] X. Li, N. Liu, H. Zhang, S. E. Knudson, R. A. Slayden, P. J. Tonge, *Bioorg. Med. Chem. Lett.* **2010**, *20*, 6306. https://doi.org/10.1016/j.bmcl.2010.08.076
[9] D. Zampieri, M. G. Mamolo, Ju Filingeri, S. Fortuna, A. de Logu, A. Sanna, D. Zanon, *Bioorg. Med. Chem. Lett.* **2019**, *29*, 2468. https://doi.org/10.1016/j.bmcl.2019.07.025
[10] G. Choudhary, R. K. Peddinti, *Green Chem.* **2011**, *13*, 3290. https://doi.org/10.1039/C1GC15701A
[11] P. K. Jaiswal, V. Sharma, J. Prikhodko, I. V. Mashevskaya, S. Chaudhary, *Tetrahedron Lett.* **2017**, *58*, 2077. https://doi.org/10.1016/j.tetlet.2017.03.048
[12] J. Petronijević, Z. Bugarčić, G. A. Bogdanović, S. Stefanović, N. Janković, *Green Chem.* **2017**, *19*, 707. https://doi.org/10.1039/C6GC02893D
[13] A. Kamal, Sh Faazil, S. M. A. Hussaini, M. J. Ramaiah, M. Balakrishna, N. Patel, S. N. C. V. L. Pushpavalli, M. Pal-Bhadra, *Bioorg. Med. Chem. Lett.* **2016**, *26*, 2077. https://doi.org/10.1016/j.bmcl.2016.02.072
[14] E. N. Kozminykh, N. M. Igidov, G. A. Shavkunova, V. O. Kozminykh, *Russ. Chem. Bull.* **1997**, *46*, 1285. https://doi.org/10.1007/BF02495929
[15] D. F. Gumerova, I. V. Mashevskaya, A. N. Maslivets, A. P. Kozlov, *Russ. J. Org. Chem.* **2003**, *39*, 995. https://doi.org/10.1023/B:RUJO.0000003192.96463.ca
[16] J.-C. Palomino, A. Martin, M. Camacho, H. Guerra, J. Swings, F. Portaels, *Antimicrob. Agents Chemother.* **2002**, *46*, 2720. https://doi.org/10.1128/AAC.46.8.2720-2722.2002
[17] N. K. Taneja, J. S. Tyagi, *J. Antimicrob. Chemother.* **2007**, *60*, 288. https://doi.org/10.1093/jac/dkm207
[18] D. Kaur, R. Kutum, D. Dash, S. K. Brahmachari, *Sci. Rep.* **2017**, *7*, 46595. https://doi.org/10.1038/srep46595
[19] H. Tomioka, Yu. Tatano, K. Yasumoto, T. Shimizu, *Expert Rev. Respir. Med.* **2008**, *2*, 455. https://doi.org/10.1586/17476348.2.4.455
[20] M. Morrison, M. R. Balmforth, S. W. Ness, D. J. Williamson, M. D. Rugen, W. B. Turnbull, M. E. Webb, *ChemBioChem* **2016**, *17*, 753. https://doi.org/10.1002/cbic.201500547
[21] Q. Sun, X. Li, L. M. Perez, W. Shi, Y. Zhang, J. C. Sacchettini, *Nat. Commun.* **2020**, *11*, 339. https://doi.org/10.1038/s41467-019-14238-3
[22] A. Scorpio, Y. Zhang, *Nat. Med.* **1996**, *2*, 662. https://doi.org/10.1038/nm0696-662
[23] V. A. Maslivets, A. N. Maslivets, *Russ. J. Org. Chem.* **2012**, *48*, 1233. https://doi.org/10.1134/S1070428012090151
[24] A. I. Kobelev, E. E. Stepanova, M. V. Dmitriev, E. S. Denislamova, A. N. Maslivets, *Russ. J. Org. Chem.* **2018**, *54*, 766. https://doi.org/10.1134/S1070428018050159

SUPPORTING INFORMATION

Additional supporting information may be found online in the Supporting Information section.

How to cite this article: Stepanova EE, Balandina SY, Drobkova VA, Dmitriev MV, Mashevskaya IV, Maslivets AN. Synthesis, in vitro antibacterial activity against *Mycobacterium tuberculosis*, and reverse docking-based target fishing of 1, 4-benzoxazin-2-one derivatives. *Arch Pharm*. 2020;e2000199. https://doi.org/10.1002/ardp.202000199